Prototype of the BDX external-veto detector: assembling and characterization

Mariangela Bondí, Marzio De Napoli, Nunzio Randazzo

September 19, 2015
V1.0
Internal Note to the BDX collaboration

1 Detector Description

The external veto system of the BDX prototype that is going to be used for cosmogenic backgroung measurements is schematically shown in Fig. 1.

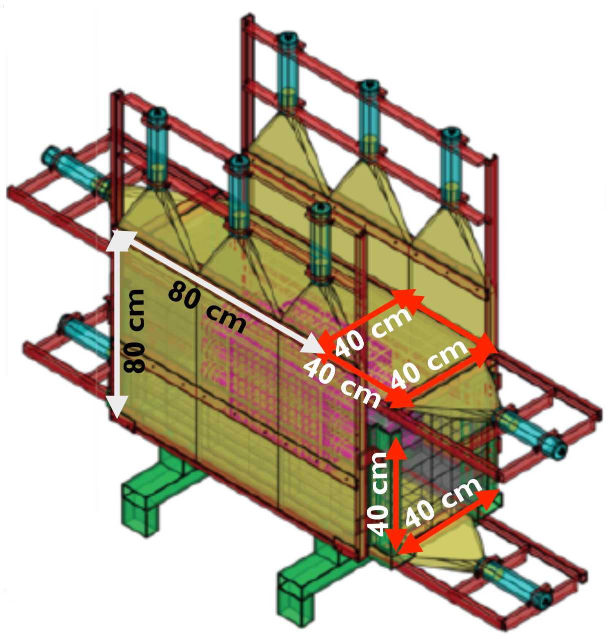

Figure 1: Schematic layout of the BDX prototype. The external veto detectors and light guides are in yellow, the PMT in blue and their mechanical supports in red.

The external veto is composed by 12 NE110 plastic scintillator detectors 2 cm thick: 8 of them with an area of 80 x 40 cm^2, the remaining 4, located one on the upper, one on the lower and two on the small later sides, with an area of 40 x 40 cm^2. Each detector is read out by a photomultiplier tube Thorn EMI 9954A 2" coupled to it through a PMMA light guide (Fig. 2), with a similar refraction index ($n_{PMMA} = 1.49$) as the the scintillator one ($n_{NE110} = 1.58$).

1.1 Wrapping and Assembling

Both scintillator and light guide were wrapped with a layer of aluminized Mylar 1.2 and 28.0 μm thick, respectively. Then for light proofing, they were covered with a layer of PROPAMETIC-701, 100 μm thick, black on one side and reflecting on the other (see Fig. 3) and black tape.
The light guide was glued to the scintillator via a bi-component glue[1] and was coupled to the photomultiplier through an optical grease[2]. Figure 4 shows the first assembled detector.

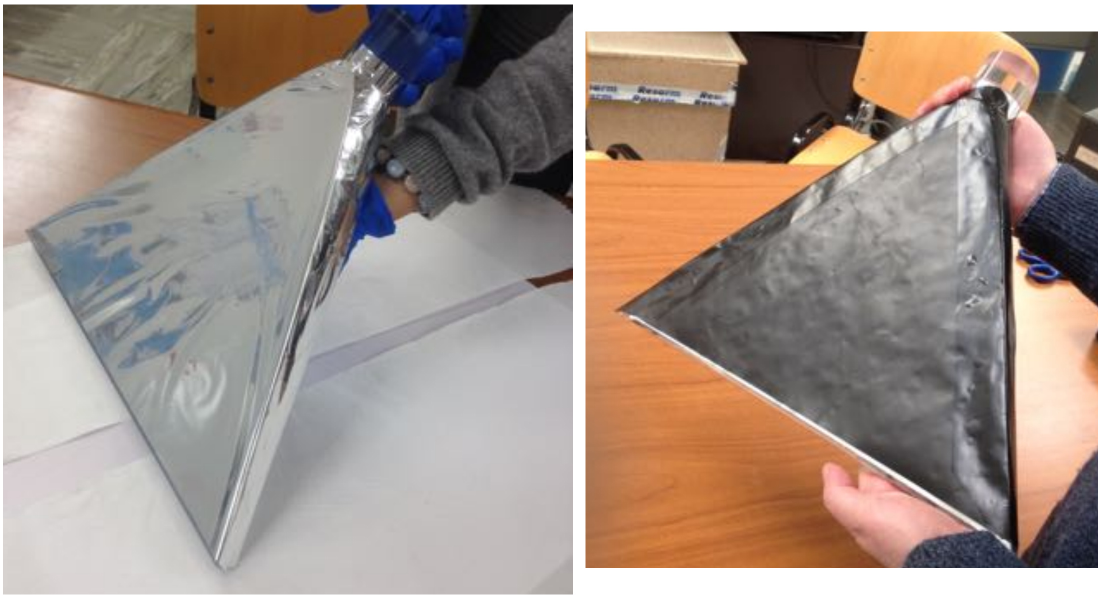

Figure 2: A light guide during wrapping.

[1] PoLytec EP 601
[2] Bysilon 300000

Figure 3: A scintillator paddle during wrapping.

Figure 4: The first assembled external-veto detector of the BDX prototype.

2 PMT characterization

Before connecting the PMTs to the light guide they were tested and the following quantities were measured: gain G, peak-to-valley ratio P/V and dark current rate.

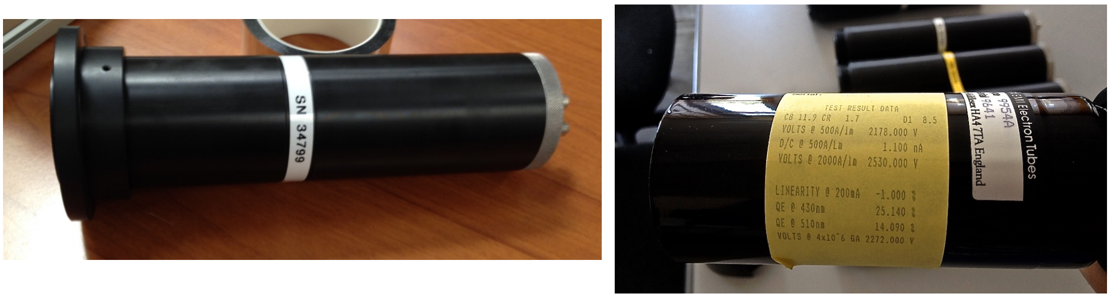

Figure 5: A phtomultiplier tube Thorn EMI 9954A 2". On each tube there is a sticker reporting some nominal quantities: quantum efficiency QE, gain, Voltage etc. In all the 15 PMT tested the reported gain at the nominal voltage is $4{\cdot}10^6$.

Since the photocatodes were exposed to light for long time, each PMT was kept in darkness without supply voltage for at least 24 h.
The PMT was powered at the nominal voltage and the single photoelectron (spe) charge spectrum was measured (Fig. 6). The amplitude of the spe signals observed with an oscilloscope terminated at 50 Ω is about 10-20 mV.
The PMT gain, i.e. the number of electrons produced per single photon hitting the photocathode, is extracted from the ratio between the mean value of the spe charge spectrum and the electron charge.
The P/V ratio is calculated as the number of counts corresponding to the centroid of the single photopeak divided by the number of counts in the lowest channel between the photopeak and the pedestal (blue arrow in Fig. 6). For the PMT 34799 of Fig. 6 we measured a gain $G \sim 2.2{\cdot}10^6$, about a factor 2 smaller than nominal one, and a $P/V \sim 3$.

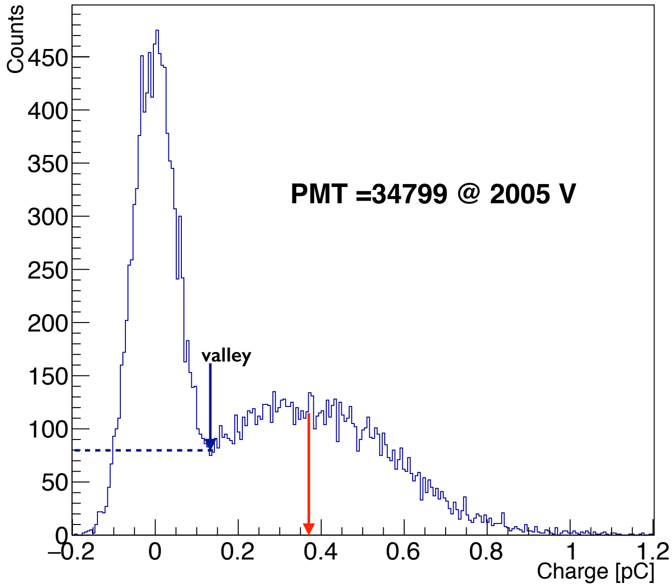

Figure 6: An example of spe charge spectrum for the PMT SN#34799 powered at the nominal voltage of 2005V. The left peak is the pedestal. The red arrow indicates the mean value of the spe centroid.

For dark current measurements we used the simple electronic chain sketched in Fig. 7 with a discriminator threshold set, when possible, to about 1/3 of the spe average pulse height.

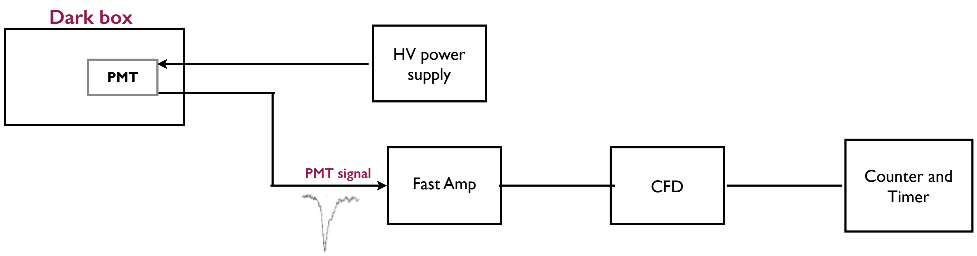

Figure 7: The electronic chain used for dark current measurements.

The results for all the 15 PMT tested are reported in Table 1.

Table 1: Summury of the results for all the 15 PMT EMI 9954A 2" tested.

Serial Number	V(Volts)	I(μA)	Dark Rate (Hz)	Gain($\cdot 10^6$)	P/V	QE(%)[a]
34655	1915	524	350	2.6	5.0	28.8
34799	2005	557	630	2.2	1.7	24.0
34784	1990	551	470	2.2	8.0	25.0
35255	1910	521	415	2.7	2.0	30.5
9796	2148	607	640	3.2	2.0	25.3
103	2130	601	700	8.0	2.0	28.9
35756	2190	625	325	6.5	1.5	30.8
9772	2011	559	625	1.8	1.6	20.4
10122	2145	609	117	3.9	3.0	26.9
10119	2141	608	85	4.5	2.5	27.9
10068	2043	570	150	1.0	8.0	27.9
34976	1850	501	1300	2.4	2.0	33.5
9850	2000	555	700	2.0	1.3	24.1
9641	2000	553	30	2.1	3.0	25.0
10324	2195	625	3000	2.0	4.0	25.0

[a] Nominal quantum efficiency of the phtocathode for a wavelenght of $\lambda = 430$ nm (Fig. 8, left). The scintillator emission wavelenght is peaked at $\lambda = 437$ nm (Fig. 8, right).

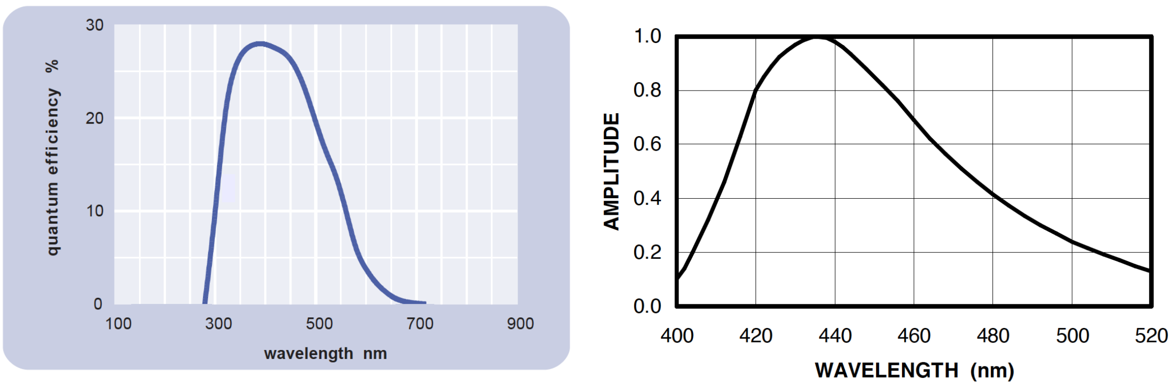

Figure 8: In the left panel, typical spectra response curves for a PMT EMI 9954[a]. In the right panel, NE110 emission spectrum[b].

[a]PMT EMI 9954 Data Sheet.
[b]EJ-208 PLASTIC SCINTILLATOR Data Sheet.

3 Detector performance

3.1 Experimental set-up

In order to investigate the performance of the detectors in terms of detection and light collection efficiency, cosmic muon measurements were performed.
Two small scintillators of 12 x 12 x 1 cm^3, hereafter called Scint_up and Scint_down, were used to trigger cosmic ray events by requiring a time coincidence between their signals. Scint_up was placed 33 cm above the BDX detector, Scint_BDX, while Scint_down 3 cm below it (Fig. 9, left). This configuration allowed to select mainly those cosmic rays crossing nearly perpendicularly the BDX detector ($\theta_{max} \sim 18°$).

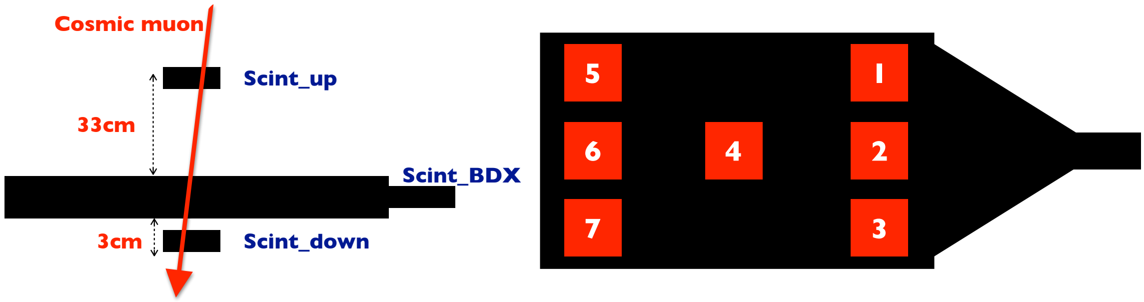

Figure 9: Sketch of the experimental set-up used for the test with cosmic rays (side-view left, top-view right). Red squares indicate the positions of the two trigger scintillators (see text for details).

In order to check possible changes in the detection and light collection efficiency as a function of the position where cosmic rays hit the Scint_BDX surface, various measurements were performed by moving the trigger detectors in 7 different positions (red squares in Fig. 9). A photo of the experiment set-up is shown in Fig. 10.
The signals of the three detectors were acquired by an oscilloscope LeCroy WwaveRunner 620Zi, whose trigger was provided by the coincidence signal between Scint_up and Scint_down. A scheme of the electronic chain is reported in Fig. 11.

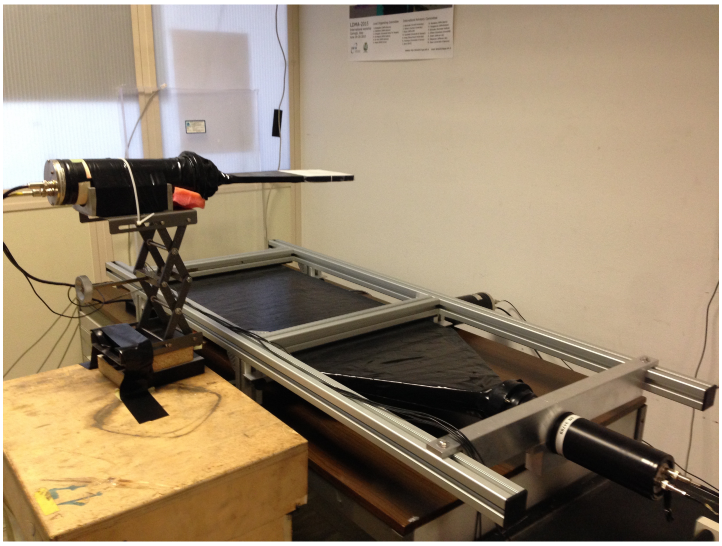

Figure 10: A picture of the experimental set-up used for the cosmic ray measurements. Scint_up and Scint_BDX are visible. This photo refers to the geometric configuration number 2 (Fig. 9, right).

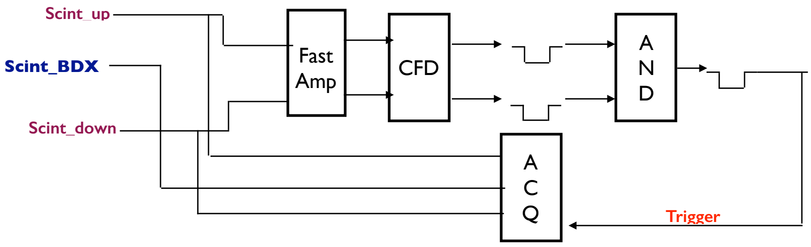

Figure 11: Scheme of the electronic chain used for the testing the BDX scintillator. Thresholds of CFD were set in order to mainly select cosmic ray events in Scint_up and Scint_down.

Typical signals of the BDX and the trigger scintillators are shown in Fig. 12. The Scint_BDX ones, yellow waveforms, are characterized by a rise time of ~ 5 ns, a fall time of ~ 40 ns and an amplitude of $\sim$ 300-400 mV. Signals do not significantly change when cosmic rays hit the detector on the 7 different surface regions we considered.

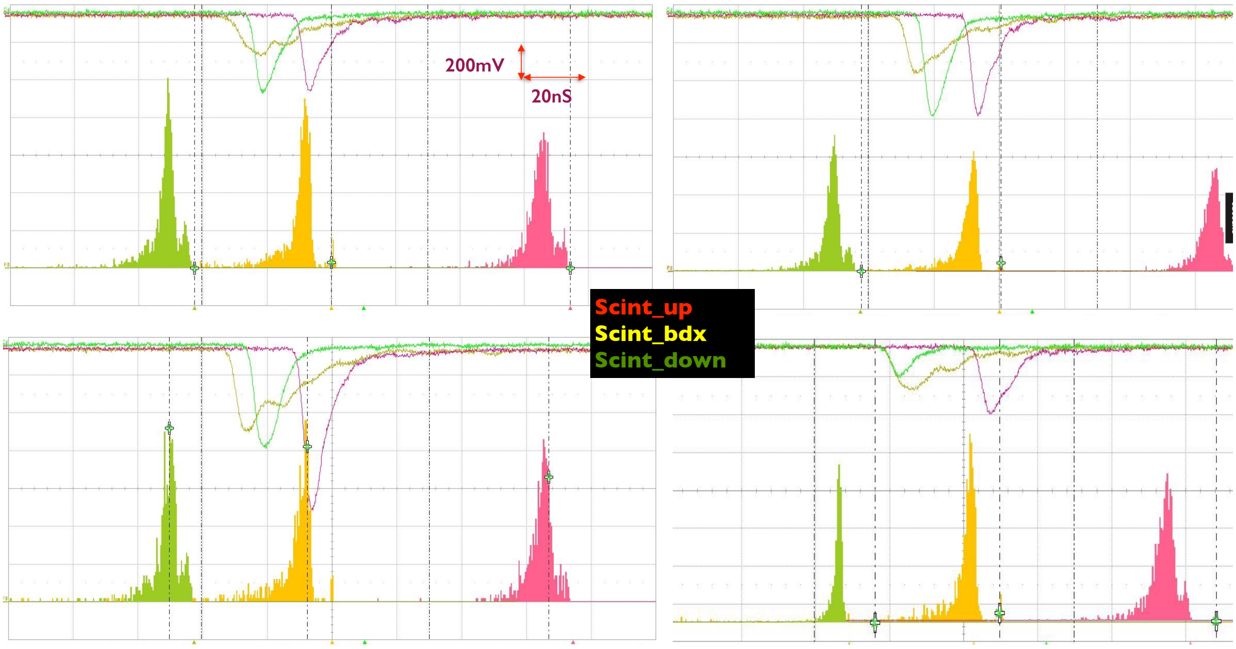

Figure 12: Example of signals acquired in the geometric configuration number 2 (Fig. 9, right). In yellow the BDX signals, in green and in red the Scint_down and Scint_up ones, respectively. The vertical scale is 200 mV/div and the horizontal one is 20 ns/div. The termination impedance of the oscilloscope was 50 Ω.

For extracting both the detection and light collection efficiency, the charge spectra of Scint_up, Scint_down and Scint_BDX were measured by integrating overtime the PMT signals. In the following we report, in details, the data analysis for the geometric configuration 2 (Fig.9, right). The same procedure was applied to the other ones.

3.2 Detection efficiency

Typical charge spectra of cosmic ray events for the three detectors, after pedestal subtraction, are shown in Fig. 13.

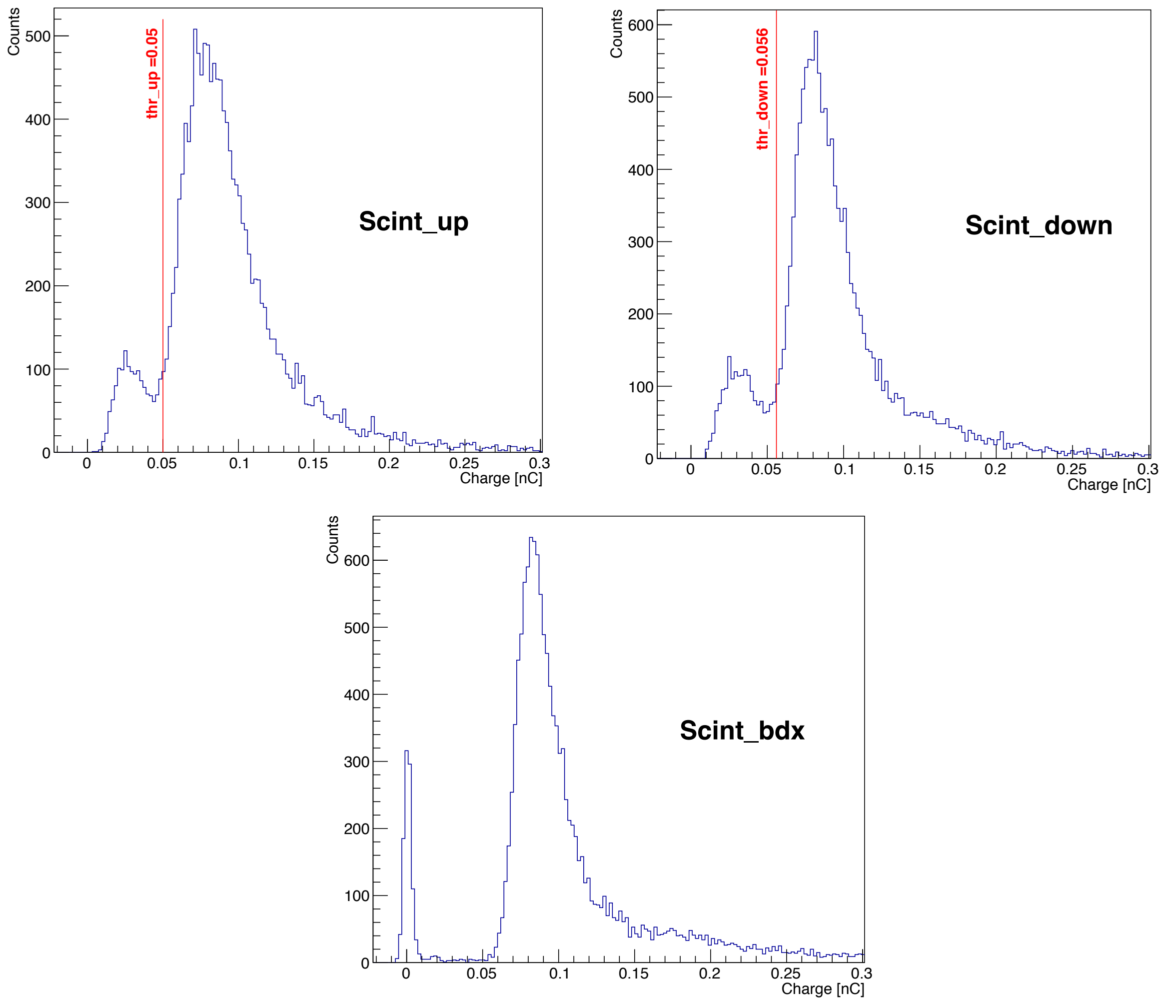

Figure 13: Typical charge spectra of cosmic ray events for the three detectors used. The red lines in the Scint_up and Scint_down spectra represent the thresholds used to cut the noise and select cosmic ray events.

The first step was to exclude from the data analysis the events due to ”fake” coincidences, i.e. coincidences generated by noise signals in one or both the trigger scintillators. For this purpose, we selected only those events where both the Scint_up and the Scint_down charge signals are higher than the thresholds reported in Fig. 13.

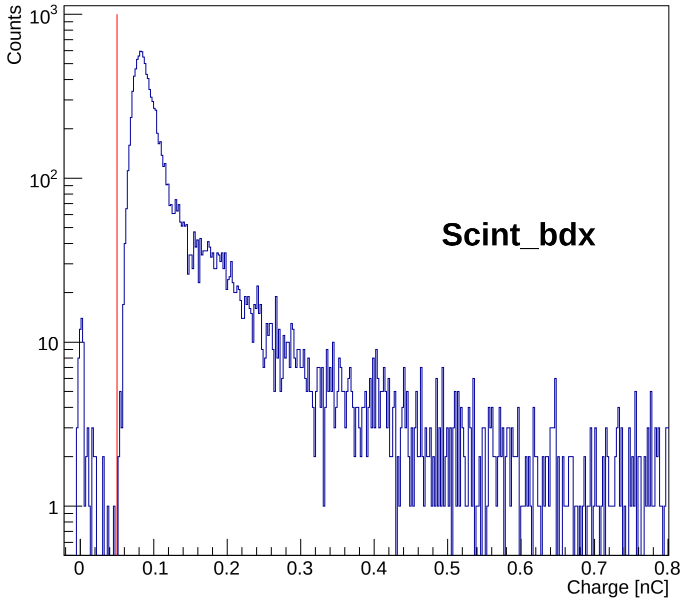

Figure 14: Scint_BDX charge spectrum of cosmic ray events obtained after cleaning the data from "fake" coincidences (see text for details). Charge signal, higher than the red line reported on the spectrum are those considered for calculating the detection efficiency.

Figure 14 shows the Scint_BDX charge spectrum for such selected events. We then calculated the detection efficiency ϵ_{det} as follows:

$$\epsilon_{det} = \frac{N_{up,down,BDX}}{N_{up,down}} \tag{1}$$

where $N_{up,down}$ is the total number of cosmic rays detected in coincidence by the trigger scintillators and $N_{up,down,BDX}$ is the number of cosmic rays observed in coincidence also in the BDX scintillator, i.e. the integral of its charge spectrum over the threshold indicated in Fig. 14. The value we found is 99.5%, with an uncertainty of $\pm 1\%$ calculated by considering just statistical errors.

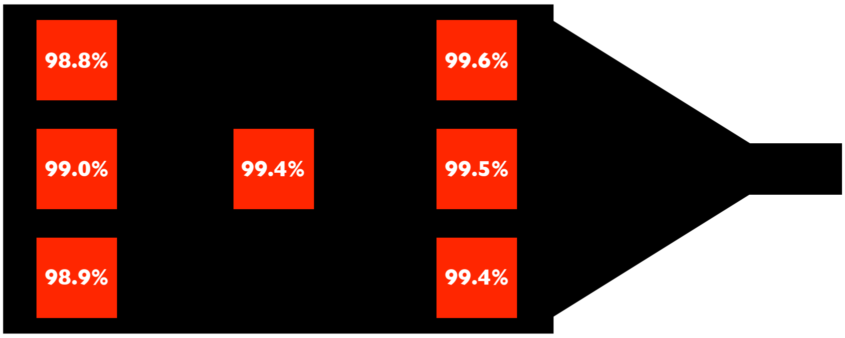

Figure 15: Summary of the detection efficiencies measured in different regions of the BDX detector surface. The uncertainty calculated by considering just statistical error is $\pm$ 1.0%.

As it can be seen from Fig. 15, the detection efficiency is constant within the uncertainty, on the whole surface of the detector.

3.3 Light Collection Efficiency L

The signal generated by a scintillator is usually quoted in terms of the number of photoelectrons produced in the PMT, that can be calculated as follows:

$$N_{phe} = dE/dx \cdot d \cdot \rho \cdot L \cdot LY \cdot QE \tag{2}$$

where dE/dx is the energy loss per unit path length of the particle crossing the scintillator, ρ is the detector density, d is the thickness of the scintillator crossed by the particle, L is the light collection efficiency, LY is the light yield of the scintillator and QE is the quantum efficiency of the photodetector.
We extracted the light collection efficiency as:

$$L = (\frac{N_{phe}^{exp}}{N_{phe}^{theo}}) \tag{3}$$

where N_{phe}^{exp} is the mean number of photoelectrons effectively measured and N_{phe}^{theo} is the number of photo-electrons expected if all the light produced in the scintillator is collected in the photocatode of the PMT.
We calculated N_{phe}^{theo}=9480 by considering muons crossing perpendicularly Scint_BDX ($d = 2$ cm) and thus depositing an energy of 4 MeV[3]. We also considered the nominal QE of 25% (Tab.1 and a LY of 9200 photons/MeV [4].

[3] dE/dx$\sim$ 2 MeV/gr/cm^2 (Particle Data Group, Review of Particle Physics) and $\rho = 1.03$ gr/cm^3 (EJ-208 PLASTIC SCINTILLATOR Data Sheet).
[4] EJ-208 PLASTIC SCINTILLATOR Data Sheet.

The mean number of photoelectrons measured is given by:

$$N_{phe}^{exp} = \frac{A_{\mu}}{A_{spe}} \tag{4}$$

where A_{μ}=0.84±0.02 nC and A_{spe} =0.36± 0.01 pC are the the centroids of the Landau functions that best-fit the Scint_BDX (Fig. 16) and the spe charge spectra, respectively. The value obtained in the geometric configuration number 2 is $L =$ (2.5 ±0.1)%, and those of other tested areas are reported in Fig. 17.

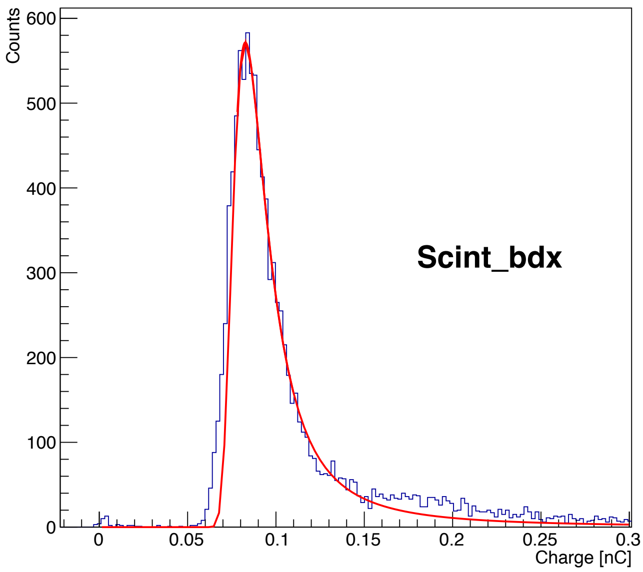

Figure 16: Best-fit of Scint_BDX charge spectrum of the cosmic rays events with a Landau function (red line).

As in the case of the detection efficiency, also the light collection efficiency is almost independent from the region of the detector surface considered.

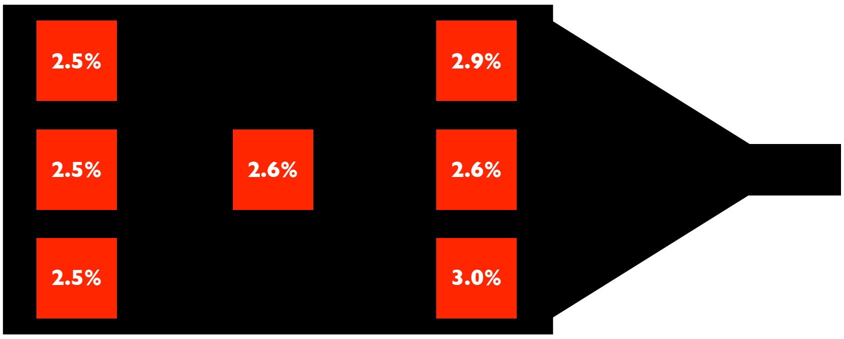

Figure 17: Summary of the light collection efficiencies measured in different regions of the BDX detector surface. The uncertainty is $\pm$ 0.1%.